complete building of mesh. Having estimated solutions timing engineer can continue to implementation phase of the decision or, if the timing is not satisfied, return to the mesh settings. Upon completion of Solutions Phase new data about solving the problem updates database of statistics, which make the following prediction more accurate.

6. Conclusion

The present method of evaluation of FEM solution time can be easily integrated into CAE system. It requires no additional computational costs small sized statistics DB storage.

Solutions time forecasting subsystem allows engineers to accurately estimate the time required for FEM analyses. If timing does not satisfy, he can return to the correction of the model before start calculation.

1. Farmaga I., Shmigelskyi P., Spiewak P., Ciupinski L. Evaluation of Computational Complexity of Finite Element Analysis // CADSM'2011, February, 23–25, Lviv, Polyana, 2011. – P. 213–214. 2. Lobur M., Farmaga I., Shmigelskyi P. Modelling of heat transfer in nanocomposites. Bulletin of the Na-tional University "Lviv Polytechnic": Computer-aided design systems. The theory and the practice. – № 711. – Lviv: "LPNU", 2011. – P. 101–104. 3. Larry J. Segerlind Appliend finite element analysis / Second Edition. John Wiley and Sons, USA, 1984.

UDK 534.231.1

P. Kosoboutskyy, M. Karkulovska
Lviv Polytechnic National University,
Institute of Computer Sciences and Information Technologies

THE REGULARITIES OF MULTIBEAM ACOUSTIC WAVES INTERFERENCE IN MEMS CAVITY-TYPE STRUCTURES WITHOUT SHEAR STRESS. ANALYSIS BY THE ENVELOPE METHOD

In this paper the amplitude-phase spectra envelope method of multi-beam acoustic waves Fabry-Perot interference in MEMS cavity-type structures without shear stress at normal and oblique beam passing limits divisions is developed. It is found that the spectra analysis by the envelope method significantly broadens the application of an appropriate approach for nondestructive testing of thin film structure parameters. In addition, on the basis of the envelope function regularities the angular conditions of Pseudo effect manifestation for the binary interface in the spectra are grounded.

Key words: MEMS-structures, Fabry-Perot interference, amplitude-phase spectra.

Розроблено метод обвідних амплітудно-фазових спектрів багатопроменевої інтерференції Фабрі-Перо акустичних хвиль для МЕМС-структур резонаторного типу без зсувних напруг при нормальному і похилому проходженні променем меж поділів. Встановлено, що аналіз спектрів методом обвідних істотно розширює межі застосування відповідного підходу для організації неруйнівного контролю параметрів плівкових структур. Крім цього, на основі закономірностей обвідних обґрунтовано кутові умови прояву в спектрах псевдобрюстерівського ефекту для бінарної межі поділу.

Ключові слова: МЕМС-структури, інтерференція Фабрі-Перо, амплітудно-фазові спектри.

Introduction

The Fabry-Perot interferometry principle was discovered in [1] and is considered to be well studied in the acoustic and optical wave ranges [2, 3]. Nowadays this approach has formed the basis for a whole class of technical solutions such as the reconstruction of parameters of heterogeneous media [4–11], sensor microelectromechanical systems (MEMS devices) [12], ensuring acoustic insulation [13], hydroacoustics [4] etc.

Some interesting regularities of the amplitude-phase Fabry-Perot spectroscopy were established in the works by [15-16]. It turned out that when the plane-parallel layer is surrounded on both sides by the media with the same characteristics (symmetric structure) the difference between the reflected and transmitted waves is $\frac{p}{2}$, and the shear of the wave phase can be determined from the experimental reflectance spectra. The method of multi-beam interference extrema envelopes has recently been developed for the optical wave range [17-21].

The aim of this work was to develop the method of multi-beam interference spectra envelopes of acoustic waves by the plane-parallel layer without shear stress and establish new principles of promising applications of this approach to the organization of non-destructive control of media parameters. Such a task has been solved for the first time.

II. The Basic Model and Main Correlations

The basic idea in the Fabry-Perot approach is the interaction between a plane or locally plane wave and a plane-parallel single-layer structure (Figure 2.1) as a spatially homogeneous one. Due to the binary interface there appears a system of coherent beams which interfere. Considering multi-beam interference the resulting amplitude reflection coefficient $\tilde{r}$ equals [2,3]:

$$\tilde{r} = \frac{\tilde{Z}_{12} + \tilde{Z}_{23}\exp\left(-i\,\tilde{d}\right)}{1+\tilde{Z}_{12}\tilde{Z}_{23}\exp\left(-i\,\tilde{d}\right)},\ \tilde{Z}_{12,23} = \frac{\tilde{Z}_{2,3}+\tilde{Z}_{1,2}}{\tilde{Z}_{2,3}-\tilde{Z}_{1,2}}. \tag{2.1}$$

Here $\tilde{Z}_{12}$ and $\tilde{Z}_{23}$ are correspondingly acoustic impedances of the media in which the wave is reflected and absorbed.

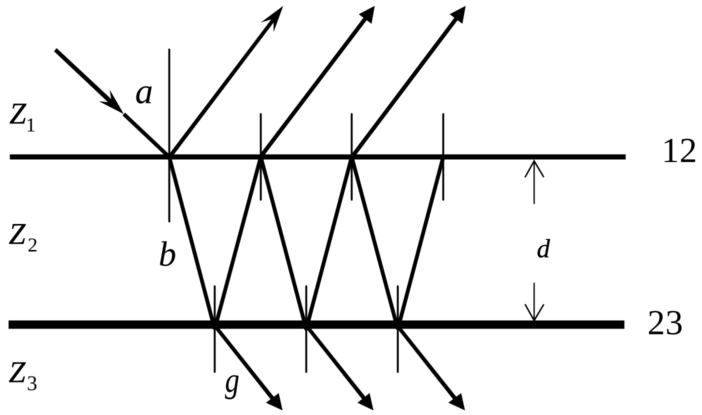

Fig. 2.1

Formula (2.1) is true at normal and oblique incidence of the interfaces by the beam if the layer does not have shear stress. In the general case, at beam incidence at the angle q_j with respect to the normal to the interface acoustic impedances of the media with the density r_j and speed of sound propagation C_j are calculated as $Z_j = \frac{r_j C_j}{\cos q_j}$ $\left(j = 1,2,3\right)$. In the case of the absorbing layer the complex speed will be calculated as $\tilde{C}_2 = \frac{C_2}{1+ih}$. In this case the shear of the plane wave phase in it equals

$$\tilde{d} = \frac{4p\,dw}{C_2}\left(1+ih\right)\cos\tilde{q}_2 = \mathrm{Re}\tilde{d} + i\,\mathrm{Im}\tilde{d}, \tag{2.2}$$

where the absorption index is considered to be h <1.

Having applied the representation of the complex number as $\tilde{Z}_{12,23} = s_{12,23} \exp\left(i f_{12,23}\right)$ and having taken the formulas of power reduction into consideration it is convenient to express the energy reflection coefficient through two envelope functions $R_{\max,\min}$ as [17-21]:

$$R = \frac{R_{\min} + b^2 \cos^2 \frac{f_{12} - \Delta}{2}}{1 + b^2 \cos^2 \frac{f_{12} + \Delta}{2}} = \frac{R_{\max} - a^2 \sin^2 \frac{f_{12} - \Delta}{2}}{1 - a^2 \sin^2 \frac{f_{12} + \Delta}{2}} . \tag{2.3}$$

Here $\Delta = f_{23} - \mathrm{Re}\tilde{d}$, $\Omega = \exp\left(\mathrm{Im}\tilde{d}\right)$, $a^2 = \dfrac{4 s_{12} s_{23} \Omega}{\left(1 + s_{12} s_{23} \Omega\right)^2}$, $b^2 = \dfrac{4 s_{12} s_{23} \Omega}{\left(1 - s_{12} s_{23} \Omega\right)^2}$,

and the functions

$$R_{\max} = \left(\frac{s_{12} + s_{23}\Omega}{1 + s_{12} s_{23}\Omega}\right)^2, \; R_{\min} = \left(\frac{s_{12} - s_{23}\Omega}{1 - s_{12} s_{23}\Omega}\right)^2 \tag{2.4}$$

are multi-beam interference spectra envelopes. In them their contact points with the Fabry-Perot contours correspond to the values $R_{\max,\min}$.

An important part in the calculation methods is the phase calculation [22]. In our work it was calculated as the tangent of the ratio $tg f = \dfrac{\mathrm{Im}\tilde{h}}{\mathrm{Re}\tilde{h}}$. Since the arctangent function is defined in the plane $\left[-\dfrac{p}{2}, \dfrac{p}{2}\right]$ for the values of the argument $z \in \left[-\infty, +\infty\right]$ its real value was calculated by the following algorithm:

1. If $\mathrm{Re}\tilde{h} > 0$ and $\mathrm{Im}\tilde{h} = 0$, then $x = 0$, and $\mathrm{Re}\tilde{h} > 0$,

   then $x = arctg\left(\dfrac{\mathrm{Im}\tilde{h}}{\mathrm{Re}\tilde{h}}\right)$, and $\mathrm{Im}\tilde{h} < 0$, then $x = 2p + arctg\left(\dfrac{\mathrm{Im}\tilde{h}}{\mathrm{Re}\tilde{h}}\right)$.

2. If $\mathrm{Re}\tilde{h} = 0$ and $\mathrm{Im}\tilde{h} > 0$, then $x = \dfrac{p}{2}$, and $\mathrm{Im}\tilde{h} < 0$, then $x = \dfrac{3p}{2}$. (2.5)

3. If $\mathrm{Re}\tilde{h} < 0$ and $\mathrm{Im}\tilde{h} > 0$, then $x = p + arctg\left(\dfrac{\mathrm{Im}\tilde{h}}{\mathrm{Re}\tilde{h}}\right)$, and $\mathrm{Im}\tilde{h} = 0$

   then $x = p$, and $\mathrm{Im}\tilde{h} < 0$, then $x = p + arctg\left(\dfrac{\mathrm{Im}\tilde{h}}{\mathrm{Re}\tilde{h}}\right)$.

III. Calculation Results, Their Analysis and Main Conclusions

The calculation of the amplitude-phase spectra envelopes was performed for the following parameter values [19]: $r_{1-3} = 1000\, kg/m^3$, $r_2 = 793\, kg/m^3$, $C_2 = 1165 m/s$, $C_{1,3} = 1483 m/s$, $h_2 = 0.01 \div 0.04$, $d = (1 \div 10) \cdot 10^{-3} m$. The analysis of the obtained results provided a possibility to draw the following most important conclusions.

3.1. Functions (2.4) are the Fabry-Perot amplitude spectra envelopes at normal and oblique incidence of the interfaces by the acoustic wave (Figure 3.1,a). The phase spectra envelopes are functions (Figure 3.1,b)

$$f_{\max,\min} = 2p + \frac{\left(1 - s_{12}^2\right) \cdot s_{23}\Omega \mp s_{12}\left(1 - s_{23}^2 \Omega^2\right) \sin f_{12}}{\pm s_{12}\left(1 + s_{23}^2 \Omega^2\right) \cos f_{12}} , \tag{3.1}$$

At that the values $R_{\max,\min}$ and $f_{\max,\min}$ do not necessarily have to coincide with the extrema vertices as by their essence they correspond to the contact points of the envelopes with the spectra contours.

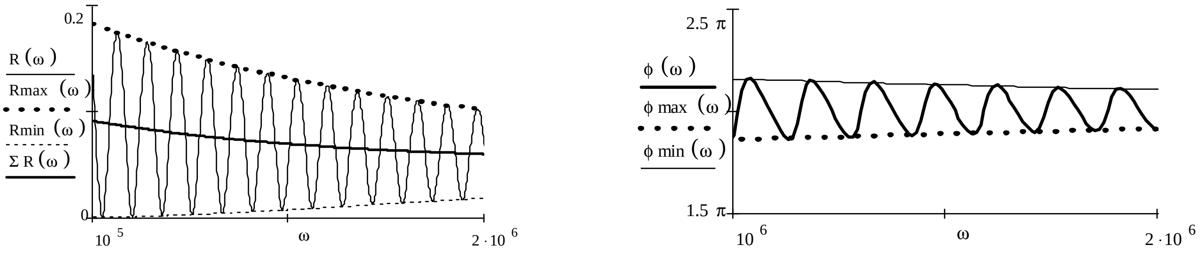

a) *b)*

Fig. 3.1

3.2. For the arbitrary geometry of experiment the ratio $\dfrac{R_{\max}-R}{R-R_{\min}}$ is changed from 0 to $+\infty$ passing at that the unit value at the frequencies w_Σ on both sides with respect to the interference maximum. At the frequencies w_Σ the value of energy reflection equals

$$\Sigma_R=\frac{1}{2}\left(R_{\max}+R_{\min}\right). \tag{3.2}$$

An analogous (3.2) condition is realized in the oblique spectrum for the angles of incidence q_Σ on both sides with respect to the interference maximum (Figure 3.1). The phase width of the reflection contour on the level (3.2) equals

$$\mathrm{H}_{\Sigma d}=\mathrm{Re}\tilde{d}\big|_{\Sigma 2}-\mathrm{Re}\tilde{d}\big|_{\Sigma 1}\cong 2\left(p-\mathrm{Re}d\big|_\Sigma\right). \tag{3.3}$$

Therefore, the experimentally measured value $H_{\Sigma d}$ provides a possibility of determining $\mathrm{Re}d\big|_\Sigma$ and the speed of sound in the layer.

3.3. An important criterion of the clarity of the interference bands is their visibility.

According to Michelson it equals $V=\dfrac{R_{\max}-R_{\min}}{R_{\max}+R_{\min}}$. Therefore, having substituted the value $R_{\max,\min}$ from (2.4) we obtain that

$$V=\frac{2}{\dfrac{s_{12}}{s_{23}\Omega}\left(\dfrac{1-s_{23}^2\Omega^2}{1-s_{12}^2}\right)+\dfrac{s_{23}^2\Omega^2}{s_{12}}\left(\dfrac{1-s_{12}^2}{1-s_{23}^2\Omega^2}\right)}. \tag{3.4}$$

We ascertain that by introducing the variable $W=\left(\dfrac{1-s_{12}^2}{1-s_{23}^2\Omega^2}\right)\dfrac{s_{23}}{s_{12}}\Omega$ we obtain the following expression for the visibility

$$V=\frac{2}{\dfrac{1}{WR}+WR}. \tag{3.5}$$

Let us establish the content of the parameter W. For this let us apply the transformation $2\dfrac{x+y}{x-y}=\dfrac{\sqrt{x}+\sqrt{y}}{\sqrt{x}-\sqrt{y}}+\dfrac{\sqrt{x}-\sqrt{y}}{\sqrt{x}+\sqrt{y}}$, as a result of which we obtain that

$$W=\frac{\sqrt{R_{\max}}-\sqrt{R_{\min}}}{\sqrt{R_{\max}}+\sqrt{R_{\min}}}. \tag{3.6}$$

In the approximation $s_{23}\Omega<<1$ the inclinations $\ln W$ and $\mathrm{Im}\tilde{d}$ coincide (Figure 3.2). Therefore, having determined the visibility of the Fabry-Perot interference bands as (3.6) we have a possibility to evaluate the complex value $\mathrm{Im}\tilde{d}$.

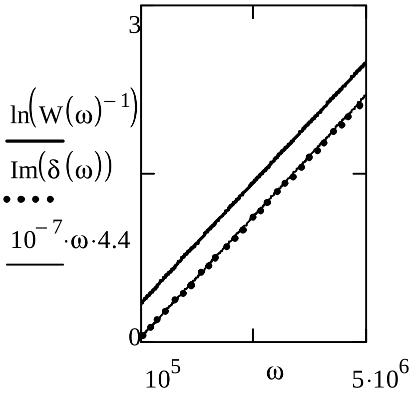

Fig. 3.2

According to the wave refraction law on the interface 12 with the absorbing medium $\frac{1}{C_1}\sin q = \frac{1}{\tilde{C}_2}\sin\tilde{q}_2$ we obtain that in the approximation $h \ll 1$ the sine of the angle of refraction can be expressed as $\sin\tilde{q}_2 = \frac{C_2}{C_1}\sin q\,\frac{1-ih}{1+h^2} \approx \frac{C_2}{C_1}\sin q\left(1-i\frac{h}{1+h^2}\right) = \sin q_2\left(1-i\frac{h}{1+h^2}\right)$, and its cosine as $\cos\tilde{q}_2 \approx \cos q_2\left(1+itg^2 q_2\frac{h}{1+h^2}\right)$. Then the complex shear of the wave phase in the layer will equal $\tilde{d} = \mathrm{Re}\tilde{d} + i\,\mathrm{Im}\tilde{d} = \frac{4p\,d}{C_2}w(1+ih)\cos\tilde{q}_2 \approx \frac{4p\,d}{C_2}w\cos q_2 + i\frac{4p\,d}{C_2}w\frac{h}{\cos q_2}$, hence its real part will be determined as $\mathrm{Re}\tilde{d} \cong \frac{4p\,d}{C_2}w\left[1-\left(\frac{C_2}{C_1}\sin q\right)^2\right]^{1/2}$ and $\mathrm{Im}\tilde{d} \cong \frac{4p\,d}{C_2}wh\left[1-\left(\frac{C_2}{C_1}\sin q\right)^2\right]^{-1/2}$. Thus in the frequency spectrum $\mathrm{Re}d\big|_{\Sigma w} = p - \frac{2p\,d}{C_2}(w_{\Sigma 2}-w_{\Sigma 1})\sqrt{1-\left(\frac{C_2}{C_1}\sin q\right)^2}$, and in the angular spectrum $\mathrm{Re}d\big|_{\Sigma q} \cong p + 4p\left(\frac{d}{C_1^2}w\right)^2 \sin(q_{\Sigma 2}-q_{\Sigma 1})\sin\left(2(q_{\Sigma 2}-q_{\Sigma 1})q_{\Sigma 1}\right)$, and the product $\mathrm{Re}\tilde{d}\cdot\mathrm{Im}\tilde{d}$ will be determined only by the level of wave absorption in the layer $\mathrm{Re}\tilde{d}\cdot\mathrm{Im}\tilde{d} \cong \left(\frac{4p\,d}{C_2}\right)^2 w^2\cdot h$. The obtained relation allows determining the index of absorption of the acoustic wave by the layer.

3.4. A criterion of the display of multi-beam interference in the spectrum is the width of the gap between the maximum and minimum envelopes [17-21]

$$\Delta R = (R_{\max} - R_{\min}) = \frac{4s_{12}s_{23}\Omega\left(1-s_{12}^2\right)\left(1-s_{23}^2\Omega^2\right)}{1-s_{12}^2 s_{23}^2\Omega^2}. \tag{3.7}$$

If the elasticities of the contacting media coincide $r_1C_1^2 = r_2C_2^2$ and $r_2C_2^2 = r_3C_3^2$ but $C_{1,3} \neq C_2$, the structure is considered to be symmetric $Z_1 = Z_3$ and this case is analogous to $p-$polarization in optics [24]. As can be seen in Figure 3.3, there is such an angle of incidence q_B at which the envelopes $R_{\max,\min}$ touch each other. At this angle of incidence $\Delta R = 0$ and multi-beam interference is not observed.

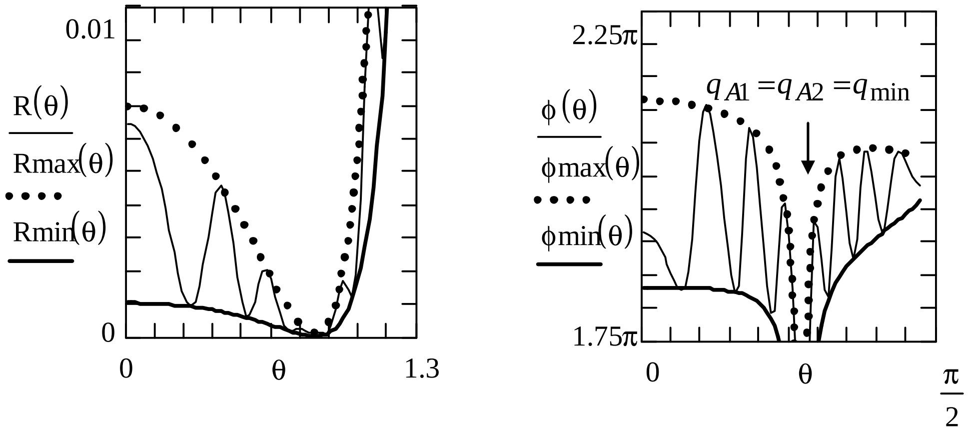

Fig. 3.3.

$$r_1 C_1^2 = r_2 \left(\mathrm{Re}\,C_2\right)^2 = r_3 C_3,\ C_1 = \sqrt{\frac{r_2}{r_1}}\,\mathrm{Re}\,\tilde{C}_2,\ C_3 = \sqrt{\frac{r_2}{r_3}}\,\mathrm{Re}\,\tilde{C}_2,\ r_1 = r_3\ i\ C_1 = C_3.$$

In its essence the angle q_B corresponds to the well-known Brewster's angle for a single interface. Since in the case of a single-film structure there are two interfaces – 12 and 23 – there can also be two angles for it – q_{B12} and q_{B23}. In the approximation $h < 1$ their values are related to the velocities of travel of the acoustic wave in the contacting media with the following relations:

$$q_{B12} \cong arc\sin\frac{C_1}{\sqrt{C_1^2 + \mathrm{Re}\,\tilde{C}_2^2}} \text{ and } q_{B23} \cong arc\sin\left(\frac{C_1}{\sqrt{\left(C_3^2 + \mathrm{Re}\,\tilde{C}_2^2\right)}}\right). \tag{3.8}$$

For the symmetric structure $q_{B12} = q_{B23}$ the described regularities of the amplitude-phase spectra of oblique reflection are presented in Figure 3.3.

Since the values of the Brewster's angles q_{B12} and q_{B23} do not depend on the real component of the phase thickness $\mathrm{Re}\,\tilde{d}$ the experimentally measured values $q_{B12,23}$ allow determining the acoustic impedance of the media which form the single-layer structure. It should be noted that like in the optical range acoustic waves are also characterized by the phenomenon of total internal reflection [25], which should also be taken into consideration at the corresponding analysis. In optics a different angular regularity of the reflection spectra is known, namely that in $s-$polarization at the increase in the angle of incidence the reflection coefficient increases gradually. For the acoustic range the corresponding analogue is the equality of the densities of the material media $r_1 = r_2$ which contact between itself [24].

3.5. The plane wave multi-beam interference in the plane-parallel layer causes the fact that at a certain angle q_{pB} the extrema minimum envelope can also display a minimum if the following equality is satisfied

$$s_{12} = \Omega s_{23}. \tag{3.9}$$

The analysis of formulas (2.4) testifies to the fact that at the angle q_{pB} the difference $\left(s_{12} - \Omega s_{23}\right)$ in the expression $R_{\min} = \left(\frac{s_{12} - s_{23}\Omega}{1 - s_{12}s_{23}\Omega}\right)^2$ changes the sign passing at that the zero value. Depending on the acoustic impedances of the media there can be several angles q_{pB}. In contrast to q_{B12} and q_{B23} at the angle q_{pB} multi-beam interference is observed but the values of q_{pB}, like q_{B12} and q_{B23}, do not depend on the phase thickness of the layer. Therefore, the angle q_{pB} can be connected with the display of the so called pseudo-Brewster's condition for the binary interface in the Fabry-Perot spectra which is a corresponding analogue of the Brewster's ones for a single interface.

3.6. The Fabry-Perot interference spectra have a $2p$ -periodicity. Therefore, the experimentally measured parameter is also the area under the contour of the reflection maximum in the gap between the two neighbouring minima which is limited at the bottom by the minima envelope which is expressed as the integral [26]

$$S_{\max} = \int R(x)\,dx - \int R_{\min}\,dx \ , \tag{3.10}$$

where $2x = \mathrm{Re}\,\tilde{d}$. Integral (3.10) is tabulated [27, formula 446.5], and it should be noted at its calculation that $R_{\min}$ and $f_{12,23}$ do not depend on the phase thickness of the layer $\mathrm{Re}\,\tilde{d}$.

1. Fabry C., Perot A. Theorie et applications d`une nouvelle methode de spectroscopie interferentielle // Ann. Chim. Phys. − 1899. − Vol. 16. − Pp. 115. 2. Brekhovskikh L.M. Acoustics in layered media. – M.: Nauka, 1973. – 343 p. (in Russian). 3. Born M.and Wolf E. Principles of Optics. New York: Pergamon, 1970. 4. Vildemar J. Paul and Foreman Terry L. A plane-wave reflection loss model including sediment rigidity // J. Acoust. Soc. Am. – 1979. – Vol. 66, № 6. – Pp. 1830–1835. 5. Nagl Anton, Uberall Herbert, Hoover William R. Resonances in acoustic bottom reflection and their relation to the ocean bottom properties. // IEEE Transactions on Geoscience and Remote Sensing. – 1982. – Vol. GE-20, № 3. – Pp. 332–336. 6. Fiorito R., Madigosky W., Uberall U. Acoustic resonances and the determination of the material parameters of a viscous fluid layer. J.Acoust. Soc.Am. – 1981. – Vol.69, № 4. – Pp. 897–903. 7. Fokina M.S., Fokin V.N. Reflection of the plane wave by an elastic layered environment: the resonant approach and numerical simulation // Acoustic magazine. – 2000. – Vol. 46, № 5. – Pp. 690-697 (in Russian). 8. Fokina M.S., Fokin V.N. Numerical simulation of reflection coefficients of the flat sound waves of layered elastic bottom // Acoustic magazine. – 2000. – Vol. 46, № 4. – Pp. 551-559 (in Russian). 9. Fokina M.S., Fokin V.N. Resonance of acoustic waves interacting with an elastic seabed // J. of Computational Acoustics. – 2001. – Vol.9, № 3. – Pp. 1079–1093. 10. Fokina M.S., Fokin V.N. Reconstruction of a layered elastic bottom characteristics by the frequency dependence of sound reflictivity // J. of Computational Acoustics. – 2001. – Vol. 9, № 4. – Pp. 1475–1484. 11. Fokina M.S., Fokin V.N. Determination of the parameters of the seabed on the frequency-angular resonances of the reflection coefficient // Acoustic magazine. – 2003.-Vol. 49, № 5. – Pp. 687-595 (in Russian). 12. International scientific-technical conferences "Sensor electronics and microsystems technology. SEMSE-1". Ukraine, Odessa, 1-5 June 2004. – Odessa: Astroprint, – 2004. – 345 p. 2004 (in Ukrainian). 13. Bogolepov I.I. Industrial soundproofing. – Leningrad: Sudostroenie, 1986. – 368 p. (in Russian). 14. Shenderov E.L. Wave processes in hydroacoustics. – Leningrad: Sudostroenie, 1972 – 352 p. (in Russian). 15. Efimov V.V., Sementsov, D.I. Phase relations for the reflection and transmission of the sound wave flat layer // Acoustic magazine. – 2001. –Vol. 47, №6. – Pp. 789 – 792 (in Russian). 16. Lobur M.V., Koosoboutskyy J.P. Determination of the phase plane of the sound wave at its passage through the layer // Acoustic journal. – 2004. – Vol. 50, № 4. – Pp. 1–2 (in Russian). 17. Kosoboutskyy P.S., Karkulovska M.S., Segeda M.S. Physical basis of simulation of wave electromagnetic processes in optics. – Lviv: NU LP, 2003. – 207 p. (in Ukrainian). 18. Kosobutskyy P.S., Morgulis A. Modelling of reflection and transmission spectroscopies of single-layer Fabry-Perrot interferometers using the envelope method, // J. Opt. Technology. Opt. Zhurn. – 2004 – Vol. 71, № 12. – Pp. 63-68 (in Russian). 19. Kosobutskyy P.S., Morgulis A. Simulation envelope method of amplitude and phase spectra of a Fabry-Perot three-layer transparent structures at normal incidence of the beam. // Ukr. J. Phys. – 2004. – Vol. 49, № 12. – Pp. 1163–1169 (in Ukrainian). 20. Kosobutskyy P.S., Morgulis A.M. Simulation envelope method of amplitude and phase spectra of the Fabry-Perot interference in the field of resonant dispersion function of dielectric permeability // Ukr. J. Phys. – 2005. – Vol. 50, № 3. – Pp. 230–233 (in Ukrainian). 21. Kosobutskyy P.S., Morgulis A.M., Danilov A.B., Karkulovska M.S. Simulation of angular regularities observed in the spectra of light reflected by three-layer plane structures with a Fabry-Perot resonator. // Ukr. J. Phys. – 2005. –

Vol. 50, № 6. – Pp. 551–555. 22. Kiselev M.I. The role of the phase and the phase of the methods in the theory and its applications // Math. Methods and phys. mech. field. – 2003. – Vol. 46, № 3. – Pp. 149–150 (in Russian). 23. Surdutovich G.I., Vitlina R. Z. and Baranauskas V. Simple reflectometric method for measement of weakly absorbing films// Thin Solid Films. – 1999. – Vol. 355–356.– Pp. 446 –450. 24. Rgevkin S.N. Lectures course on the theory of sound. – M: Moscow State University, 1960. – 335 p. 25. Podilchuk U. N., Rubczov U.K. Ray methods in the theory of propagation and scattering of waves.. – Kyiv: Naykova dumka, 1988. – 220 p. 26.Kosoboutskyy P.S., Karkulovska M.S., Kosoboutskyy J.P. On phase-amplitude correlation in reflection spectra of Fabry-Perrot interferometers // Optica and Spectroscopy. – 2003. – Vol. 94, № 3. – Pp. 434–436. 27. Dwigt H.B. Tables of Integrals and other Matematical Data. 4nd ed. New York, The Mac Millan Company.1961.

UDK 811.161.2

M. Lobur, A. Romaniuk, M. Romanyshyn
Lviv Polytechnic National University
Computer-Aided Design Department

DEFINING AN APPROACH FOR DEEP SENTIMENT ANALYSIS OF REVIEWS IN UKRAINIAN

This paper studies the approaches commonly used for sentiment analysis and defines an optimal approach for Ukrainian language analysis.

Key words: rule-based sentiment analysis, deep sentiment analysis, sentiment dictionaries.

Описано підходи до емоційно-смислового аналізу, а також визначення найкращого підходу для української мови.

Ключові слова: емоційно-смисловий аналіз на основі правил, глибокий емоційно-смисловий аналіз, тональні словники.

1. Problem

Sentiment analysis is the task of natural language processing, which is widely used nowadays in such areas as sociology (e.g. collecting data from social networks about people's likes and dislikes), political science (e.g. collecting data about political views of certain social groups), marketing (e.g. creating ratings of products/companies/people), medicine and psychology (e.g. detecting signs of psychological illnesses or signs of depression in users' messages, detecting bullies with the help of messages in microblogs, like Twitter), etc. [1].

Unfortunately, no matter how useful such a tool would be, there is no available sentiment analysis system for Ukrainian language yet. The aim of this paper is to study the most effective approaches to sentiment analysis and thus find the optimal approach for implementing such an analyser for Ukrainian. The approaches researched in this paper include a rule-based approach, statistical analysis based on sentiment dictionaries and approaches based on machine learning algorithms.

2. Recent Research Analysis

The previous decade showed a rising interest in the area of sentiment analysis. This has been proven with a large number of projects, which appear every day: sentiment analysis of hotel reviews [9], bank reviews [5], restaurant reviews, comments on movies [21], products, messages about political events in blogs and social networks, etc. A big number of studies are dedicated to sentiment analysis of messages in microblogs (e.g. Twitter, Google Buzz).